THE JOURNAL OF BIOLOGICAL CHEMISTRY VOL. 288, NO. 36, pp. 25804–25809, September 6, 2013

Ganglioside GM1-mediated Transcytosis of Cholera Toxin Bypasses the Retrograde Pathway and Depends on the Structure of the Ceramide Domain*

Received for publication, April 5, 2013, and in revised form, June 26, 2013 Published, JBC Papers in Press, July 24, 2013, DOI 10.1074/jbc.M113.474957

David E. Saslowsky[‡§¶1], Yvonne M. te Welscher[‡¶], Daniel J.-F. Chinnapen[‡¶], Jessica S. Wagner[‡§], Joy Wan[‡], Eli Kern[‡], and Wayne I. Lencer[‡§¶]

From the [‡]Division of Gastroenterology, Boston Children's Hospital, [§]Harvard Digestive Diseases Center, and [¶]Harvard Medical School, Boston, Massachusetts, 02115

Background: Mechanisms for intracellular lipid sorting remain poorly understood.
Results: Polarized epithelial cells sort ganglioside GM1, the receptor for cholera toxin, into distinct retrograde and transcytotic pathways, provided that GM1 contains ceramide domains with short or unsaturated fatty acid chains.
Conclusion: Sphingolipid sorting depends on ceramide structure, implicating a mechanism for lipid sorting by lipid shape.
Significance: The results identify a lipid-sorting pathway across epithelial barriers with clinical applications.

Cholera toxin causes diarrheal disease by binding ganglioside GM1 on the apical membrane of polarized intestinal epithelial cells and trafficking retrograde through sorting endosomes, the trans-Golgi network (TGN), and into the endoplasmic reticulum. A fraction of toxin also moves from endosomes across the cell to the basolateral plasma membrane by transcytosis, thus breeching the intestinal barrier. Here we find that sorting of cholera toxin into this transcytotic pathway bypasses retrograde transport to the TGN. We also find that GM1 sphingolipids can traffic from apical to basolateral membranes by transcytosis in the absence of toxin binding but only if the GM1 species contain *cis*-unsaturated or short acyl chains in the ceramide domain. We found previously that the same GM1 species are needed to efficiently traffic retrograde into the TGN and endoplasmic reticulum and into the recycling endosome, implicating a shared mechanism of action for sorting by lipid shape among these pathways.

Cholera toxin (CT)[2] secreted by *Vibrio cholerae* typifies the structure and function of AB_5 subunit toxins that intoxicate host cells by moving retrograde from the cell surface through endosomes and the trans-Golgi network (TGN) into the endoplasmic reticulum (ER). For CT, this requires binding of its B subunit to the ganglioside receptor GM1, which acts as the vehicle for retrograde trafficking into the TGN and ER (1). Once in the ER, a portion of the A subunit is unfolded and retrotranslocated to the cytosol to induce toxicity. The pentameric structure of the CT B subunit allows for binding of five GM1 molecules simultaneously. Such cross-linking of GM1 affects trafficking of the CT-GM1 complex, enhancing the efficiency of retrograde transport and the induction of disease (1–3).

In nature, *V. cholerae* colonizes the intestine, and CT enters the host through the apical membrane of polarized epithelial cells that line the intestinal lumen. These cells form the robust but delicate single-cell barrier against passive diffusion of small and large solutes, macromolecular complexes, and microorganisms, essential for intestinal function and host defense. In studying how CT enters the apical membrane of polarized epithelia, we found that, in addition to retrograde transport, binding to GM1 also allows CT to cross the epithelial cells from the apical to the basolateral surface by transcytosis (4), thus enabling CT to breach the intestinal barrier as an intact protein. In principle, the CT-GM1 complex could traffic across polarized cells by virtue of its ability to efficiently sort retrograde into the TGN and ER, from where it could move to the contralateral cell surface within anterograde transport vesicles of the secretory pathway that normally emerge from these compartments. We have found evidence for and against this hypothesis (4, 5).

Almost nothing is known about the itinerary or mechanism of membrane sorting in the absorptive basolaterally directed transcytotic pathway. The Fcγ receptor FcRn is the only other known membrane receptor that moves cargo efficiently from apical to basolateral membranes by transcytosis (6). Although a key sorting step appears to occur in the common sorting endosome of polarized cells (7, 8), how FcRn sorts IgG into the transcytotic pathway remains poorly understood. In polarized cells, the common endosome functions in many ways like the sorting endosome of non-polarized cells (9). It receives membrane and fluid-phase cargo internalized from both apical and basolateral cell surfaces and distributes cargo among the recycling, retrograde, and (uniquely to polarized cells) transcytotic pathways. The common endosome also delivers cargo to the lysosome by

* This work was supported, in whole or in part, by National Institutes of Health Grants R01 DK48106, R01 DK084424, and R21 DK090603 (to W. I. L.); K01 DK073480 (to D. E. S.); and P30 DK34854 (to the Harvard Digestive Diseases Center). This work was also supported by a Boston Children's Hospital Career Development Award (to D. E. S.).
[1] To whom correspondence should be addressed: Division of Gastroenterology, Boston Children's Hospital, 300 Longwood Ave., Enders Bldg. RM 609, Boston, MA 02115. Tel.: 617-919-2550; Fax: 617-730-0498; E-mail: david.saslowsky@childrens.harvard.edu.
[2] The abbreviations used are: CT, cholera toxin; TGN, trans-Golgi network; ER, endoplasmic reticulum; MDCK, Madin-Darby canine kidney; IP, immunoprecipitation; BFA, brefeldin A; CTB, cholera toxin B subunit; CTB-GS, cholera toxin B subunit with glycosylation and sulfation motifs; PM, plasma membrane.

active (ESCRT, endosomal sorting complex required for transport) or passive retention within the maturing endosome (10, 11).

Here we elucidate the intracellular itinerary for transcytosis of CT across polarized epithelial cells grown in monolayer culture. We used a mutant toxin (CTB-*GS*) containing *N*-glycosylation and tyrosine-sulfation motifs to report on retrograde transit through the TGN and ER, respectively (12), and selective biotinylation of basolateral cell surface proteins to track the fraction of toxin crossing the cell by transcytosis. We found that the retrograde and transcytotic pathways do not intersect, implicating distinct itineraries and the early/common endosome as the site for GM1 lipid sorting. We also found that efficient sorting of GM1 into the transcytotic pathway does not require cross-linking by toxin binding, providing that the GM1 species contain *cis*-unsaturated or short acyl chains in the ceramide domain.

EXPERIMENTAL PROCEDURES

Reagents and Cell Culture—CT was obtained from Calbiochem, and CT-GS was as described (12). Polyclonal rabbit anti-CTB was as described (5). HRP-conjugated secondary antibodies and sulfo-NHS-biotin were from Thermo Scientific. Radioactive ^{35}S was from PerkinElmer Life Sciences. Polarized monolayers of T84 and MDCK II cells were cultured on 0.33 or 5 cm^2 polyester Transwell® inserts (Corning) as described previously (4).

TGN/ER Trafficking Assay and Selective Cell Surface Biotinylation—A mutant CT (CT-GS) harboring sulfation and glycosylation motifs appended to the C terminus of CTB has been described previously (12). Basolateral or apical surfaces of polarized T84 monolayers were selectively biotinylated as described (4).

Immunoprecipitation and Affinity Precipitation—Transwell filters were excised into lysis buffer (20 mM Tris (pH = 8), 150 mM NaCl, 5 mM EDTA, 20 mM triethanolamine, 0.5% SDS, 0.2% BSA, and complete protease (Roche)), heated at 100 °C for 10 min, and diluted to accommodate immunoprecipitation (IP). IP of CTB was as described before (13), and some samples were then affinity-purified of biotin conjugates using NeutrAvidin®-agarose (Thermo Scientific). SDS-PAGE, Western blot analysis, and phosphorimaging was as described (13).

GM1 Lipid Synthesis and Alexa Fluor Labeling—GM1 species were covalently labeled with Alexa Fluor 568 (Invitrogen) and purified by HPLC as described previously (1).

Transcytosis Conditions—High electrical resistance T84 monolayers or MDCK II cells were washed in Hanks' balanced salt solution (HBSS) (pH = 7.4) for all experiments. For Alexa Fluor-conjugated GM1 experiments, apical surfaces of inverted-grown monolayers were equilibrated for 15 min at 10 °C with HBSS containing 0.034% defatted BSA and then incubated apically with either 1.2 μM C16:1, 2 μM C16:0, or 0.8 μM C12:0 Alexa Fluor-labeled GM1 (in HBSS + 0.034% defatted BSA) for 1 h at 10 °C. Monolayers were then warmed to 37 °C or kept at 4 °C for 2 h for MDCK II and 3 h for T84 cells, washed in HBSS, and imaged live by confocal microscopy as described below.

Biochemical Quantitation of GM1 Transcytosis—MDCK II monolayers grown on 12-well inserts were incubated with unlabeled GM1 species as above (1.2 μM C16:1 or 2 μM C16:0; continuous incubation during the 2-h 4 °C or 37 °C step). Some monolayers were treated with 10 μM BFA for 20 min prior to and during apical GM1 incubation. Monolayers were returned to 4 °C and incubated basolaterally with 10 nM CTB for 30 min on ice. After extensive washing, monolayers were lysed (2 filters combined/sample), and CTB was immunoprecipitated as before (5), separated by SDS-PAGE, detected by immunoblot analysis, and then bands were quantified using a ChemiDoc XRS^+ imaging system (Bio-Rad).

Measurement of PM GM1 Loading—Apical surfaces were equilibrated at 10 °C with HBSS/0.034% BSA. Monolayers were incubated apically with either 1.2 μM C16:1 or 2 μM C16:0 Alexa Fluor-labeled GM1 in HBSS/BSA for 1 h at 10 °C, washed, incubated apically ± 0.25% trypsin on ice for 5 min, washed, and then inserts were excised into 100-μl, 37 °C radioimmune precipitation assay buffer for 10 min (25 mM Tris-HCl (pH 7.4), 150 mM NaCl, 1% Nonidet P-40, 1% sodium deoxycholate, 0.1% SDS). Lysates were spun at 6000 × *g* for 20 min, and supernatant fluorescence was measured using a FLUOstar Omega plate reader (excitation, 544 nm; emission, 620 nm; BMG Labtech).

Fluorescence Microscopy—Confocal images were collected using either a Nikon PlanApo ×100 (1.4 numerical aperture) or a PlanFluor ×40 (1.3 numerical aperture) lens on a Nikon TE2000 inverted microscope coupled to a PerkinElmer spinning disk confocal unit and an Orca AG cooled charge-coupled device camera (Hamamatsu Photonics K.K.). Slidebook software (Intelligent Imaging Innovations, Inc.) was used for image capture and processing.

RESULTS

To define the intracellular itinerary of CT during transcytosis, we applied CTB-GS to apical surfaces of intestinal T84 cell monolayers preincubated with ^{35}S-sulfate (13, 14). After 2 h, the monolayers were cooled to 4 °C, washed extensively, and basolateral membrane and membrane-associated proteins were selectively tagged with biotin as described previously (4). CTB-GS was then either immunoprecipitated from total cell lysates using an anti-CTB antibody (Fig. 1, *A* and *B*, *lane 1*) or double affinity-purified by immunoprecipitation followed by "pull-down" with avidin-coupled beads to isolate the fraction of CTB-GS that had been transcytosed, as evidenced by the biotin tag (Fig. 1, *A* and *B*, *lane 2*). Both fractions were analyzed by SDS-PAGE followed by immunoblot analysis (Fig. 1*A*) and autoradiography (*B*) to quantify the fraction of ^{35}S-sulfate-labeled toxin that had transited through the TGN and ER.

Equal amounts of CTB-GS were loaded for analysis (Fig. 1*A*, *uppermost band* in *lanes 1* and *2*). A fraction of total cell-associated CTB-GS was ^{35}S-radiolabeled, indicating transit through the TGN (Fig. 1*B*, *lane 1*, *lower band*) or through the TGN and ER (*upper band* marked by *asterisk*, representing *N*-glycosylation of the CT B subunit as described (14)). No ^{35}S-radiolabeled toxin, however, was detected in the transcytosed fraction of CTB-GS that was tagged with biotin on the basolateral membrane (Fig. 1*B*, *lane 2*). Transport to the basolateral membrane did not occur by paracellular diffusion because no basolaterally biotinylated CTB-GS was detected in control monolayers incubated continuously at 4 °C and studied in parallel (Fig. 1*C*). We

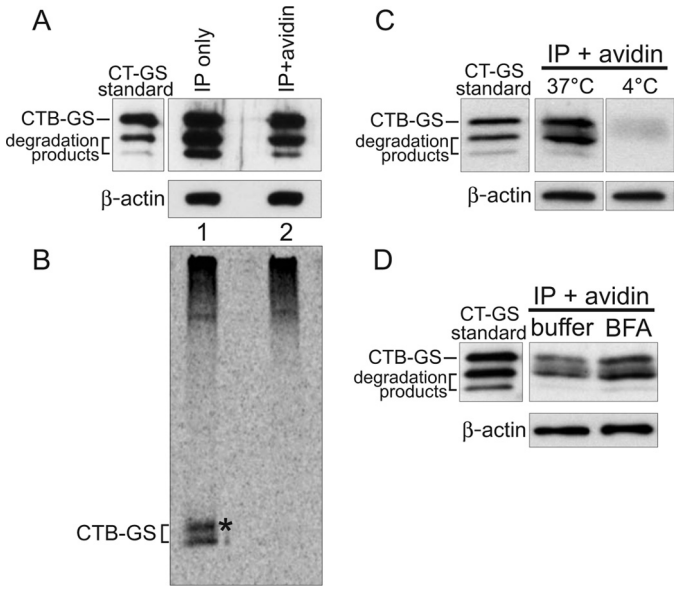

FIGURE 1. **Sorting of CT into the transcytotic pathway bypasses retrograde transport to the TGN and ER.** *A–D,* polarized T84 monolayers were incubated apically with 10 nM CT-GS for 2 h at 37 °C prior to biotinylation of the basolateral surfaces. Total toxin was immunoprecipitated from cell lysates and either analyzed directly (*IP only*, captures all CT-GS) or subjected to an additional avidin affinity purification step (*IP + avidin*, captures only basolateral CT-GS). To achieve similar CTB-GS levels between the total and basolateral pools, 7-fold more cells were used for the IP + avidin samples. 10% of each sample was analyzed by SDS-PAGE and immunoblot analysis using anti-CTB (*A*), with the remainder being separated by SDS-PAGE and analyzed by autoradiography (*B*). Pure CT-GS is indicated (*standard*), and crude lysates were separated by SDS-PAGE and probed with an antibody against β-actin as a loading control (*A*, *C*, and *D*, *lower panels*). The *asterisk* in *B* denotes a higher molecular weight glycosylated CTB-GS band. *C*, T84 monolayers were treated as in *A*, except cells were not pretreated with ^{35}S-sulfate, and some cells were held at 4 °C during the 2-h apical toxin incubation. Basolateral CT-GS fractions (*IP + avidin*) were immunoblotted using anti-CTB. *D*, as in *C*, except cells were incubated with either buffer or 10 μM BFA for 20 min prior to apical exposure to 10 nM CT-GS for 2 h at 37 °C. Data are representative of three independent experiments for *A–C* and two independent experiments for *D*.

also found that blockade of retrograde trafficking to and from the ER by pretreatment of cells with brefeldin A (BFA) failed to block transcytosis of CTB-GS (Fig. 1*D* and Ref. 4). Transcytosis of CTB-GS was slightly enhanced by BFA, as we observed previously (4), which may indicate greater amounts of CTB available within the early sorting endosomes for entry into the transcytotic pathway because of the block in retrograde transport. Thus, the fraction of CTB-GS that crosses the cell by apical-to-basolateral transcytosis does not enter the TGN or ER en route to the basolateral membrane. The result implicates the "common endosome" (8, 9, 15) as the site for sorting between the two pathways.

We found recently that the structure of the ceramide domain of GM1, the lipid portion of GM1 anchoring the molecule in the membrane, dictates the efficiency of its trafficking in the retrograde pathways from PM to the TGN and ER in the absence of cross-linking by CTB (1). To test whether transcytosis of GM1 is also independent of toxin cross-linking and to test whether the ceramide structure of GM1 affects sorting into the transcytotic pathway, we used the same GM1 species employed in our earlier studies. Briefly, distinct GM1 lipids were synthesized to contain ceramide domains differing only in the structure of their acyl chains (C12:0, C16:0, or C16:1) and with Alexa Fluor 568 attached to the extracellular oligosaccharide head group (1). Each of these Alexa Fluor-labeled GM1 species were introduced into apical membranes of either polarized canine kidney MDCK or human intestinal T84 monolayers and analyzed in live cells for transcytosis to the basolateral membrane by confocal microscopy.

We found that by 2 h at 37 °C, the Alexa Fluor-labeled GM1 species harboring a single *cis*-unsaturated 16-carbon acyl chain in the ceramide domain (C16:1-GM1) was transported from the apical to the basolateral membranes (Fig. 2, *D* and *E*). No basolateral membrane localization was detected in control monolayers incubated at 4 °C (Fig. 2, *J* and *K*), indicating that transcellular GM1 transport was by transcytosis and not paracellular diffusion. In contrast to C16:1-GM1, a much smaller amount of the GM1 species containing saturated C16:0 acyl chains was transported to the basolateral surface (Fig. 2, *G* and *H*), although comparable levels of the two sphingolipids were initially incorporated into the apical PM, as assessed by biochemistry and microscopy (*B*, *C*, *F*, and *I*). Similar results were obtained when C16:1-GM1 and C16:0-GM1 species were applied to intestinal T84 monolayers, although transepithelial transport in T84 cells was often weaker than in MDCK cells and typically required longer incubation times for detection (Fig. 2, *L–N*). GM1 species with a short C12:0 ceramide chain were rapidly and greatly transported across T84 monolayers, suggesting that this short-acyl chain ceramide sorts more efficiently into the transcytotic pathway than either C16:1-GM1 or C16:0-GM1 (Fig. 2*O*).

To quantify the relative amount of apical-to-basolateral transcytosis for the different GM1 species, we measured the binding of CTB to basolateral membranes of MDCK monolayers, as assessed by immunoblot analysis (Fig. 3). Although indirect, this method is the most accurate means to gauge GM1 levels in only the basolateral PM. MDCK II cells not treated apically with exogenous GM1 had very low levels of CTB bound to basolateral membranes, indicative of low levels of endogenous GM1 (Fig. 3, *BSA only*, *lane 3*). Monolayers treated apically with either C16:1-GM1 or C16:0-GM1 species and incubated at 4 °C had weak signals for CTB binding to basolateral membranes, only slightly above BSA control background levels and perhaps indicative of a small paracellular leak (Fig. 3, *lanes 1* and *2*). Monolayers incubated apically for 2 h at 37 °C with the C16:1-GM1 species, however, had strong signals for CTB binding to basolateral membranes (Fig. 3, *lane 5*). This was enhanced (~40%) by pretreating the cells with BFA (Fig. 3, *lane 6*), consistent with our results for transcytosis of CTB-GS across intestinal T84 monolayers (Fig. 1*D*). In contrast, monolayers incubated apically with the C16:0-GM1 species displayed much less GM1 transport, binding over 3-fold less CTB on basolateral membranes when compared with monolayers treated with the C16:1-GM1 species (Fig. 3, compare *lanes 4* and *5*). Thus, GM1 containing C16:1 unsaturated fatty acids trafficked across MDCK monolayers more efficiently than the GM1 species with C16:0 ceramide domains, consistent with our previous results obtained by microscopy (Fig. 3). These results implicate a sorting mechanism dependent upon lipid shape (1).

In the retrograde pathway from PM to ER, sorting of GM1 depends on the lipid raft-associated protein flotillin (14). To

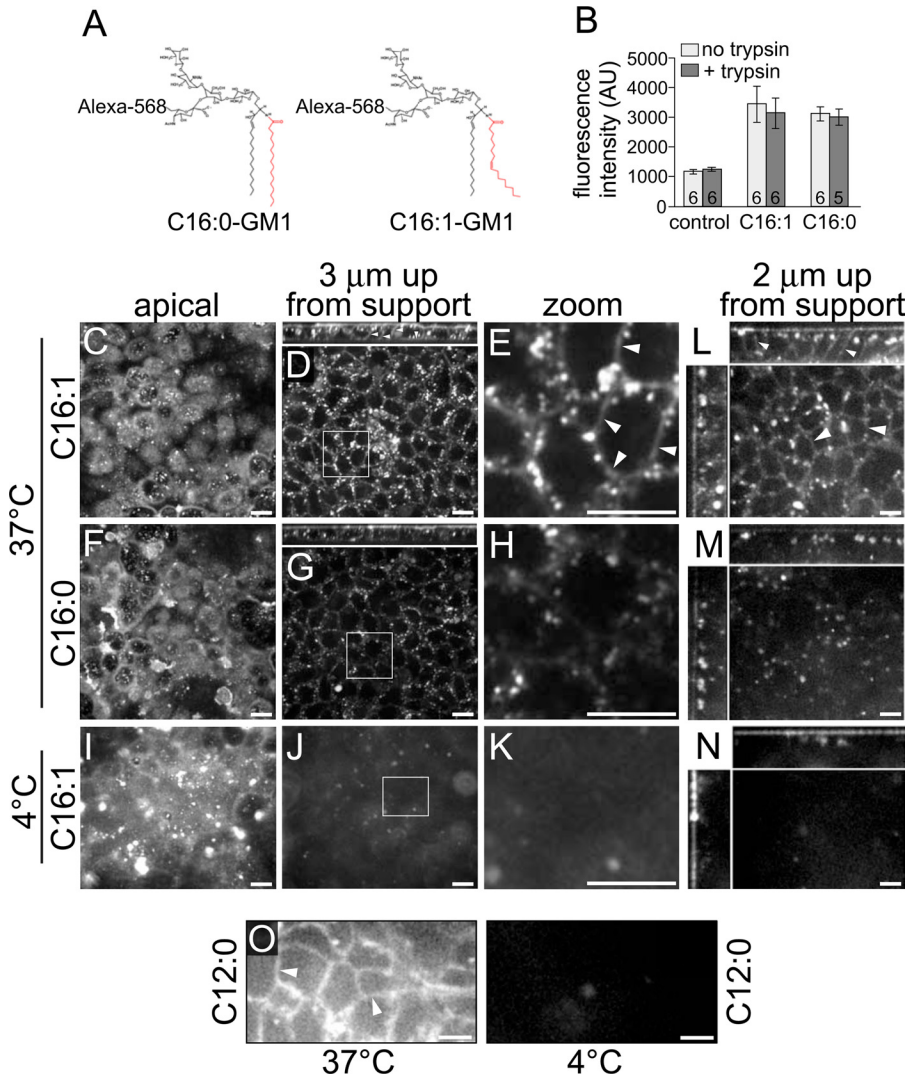

FIGURE 2. **Polarized epithelial cells sort GM1 gangliosides into the basolaterally directed transcytotic pathway on the basis of the structure of the ceramide domain.** *A*, schematic of GM1 structures. *B*, cell lysates of MDCK monolayers preincubated with the indicated Alexa Fluor-labeled GM1 species were measured by fluorimetry and reported as arbitrary units (*AU*) of fluorescence (± S.E.). The number of monolayers/condition is indicated at the column base. *C–O*, polarized epithelial monolayers were incubated apically with the indicated fluorophore-labeled GM1 species at 10 °C for 1 h, shifted to either 37 °C or 4 °C for the times indicated below, and imaged live by confocal microscopy. *C–K*, MDCK monolayers were incubated for 2 h at the indicated temperatures and imaged at the indicated *Z* plane (*small panels* above *D* and *G* show *X-Z* reconstructions). Zoomed images (*E, H,* and *K*) are from *insets* in *D, G,* and *J. L–O*, T84 monolayers were incubated apically with the indicated GM1 species for 3 h at the temperatures shown. *Main panels in L-N* are *X-Y* optical sections imaged 2 μm up from the basolateral support, and *small panels* at the *top* and *left* are *X-Z* and *Y-Z* reconstructions, respectively. *O*, T84 monolayers were incubated with Alexa Fluor-conjugated C12:0-GM1 at the indicated temperature and imaged 2 μm up from the basolateral support. *Arrowheads* indicate basolateral membrane labeling in *E, L,* and *O*. *Scale bars* = 10 μm. Data are representative of three independent experiments for *B* and *O* and at least six independent experiments for *C–N*.

test whether flotillin also operates in the transcytotic pathway, we used polarized T84 cell monolayers stably expressing shRNA against flotillin 1 and with > 85% depletion of the protein. T84 monolayers expressing a non-targeting shRNA were used as controls. To assess the retrograde pathway from PM to ER, we measured CT-induced toxicity, which is fully dependent on the transport of toxin into the ER for retrotranslocation of the CT A1 chain to the cytosol. In contrast to the ~85% decrease in retrograde ER transport observed in non-polarized monkey Cos-1 cells (14), stable flotillin depletion in intestinal T84 cells caused only a small block in CT-induced toxicity (~35% decrease). Flotillin 1 depletion had no detectable effect on transcytosis of C16:1-GM1 or C16:0-GM1, as assessed by confocal microscopy (not shown), suggesting that flotillin may not be involved. It is possible, however, that flotillin depletion has a small effect on sorting GM1 into the transcytosis pathway that is below detection by our methods.

DISCUSSION

The results of these studies show that, in polarized epithelial cells, sorting of GM1 gangliosides into the basolaterally directed transcytotic pathway is, at least in part, on the basis of the structure of the ceramide domain. Cross-linking multiple GM1 molecules together by the CT B subunit is not necessary for GM1 transcytosis, indicating an endogenous pathway of sphingolipid transport, as implied by previous studies (15). Sorting of GM1 into the transcytotic pathway appears to occur before or within the early apical or common endosome of polar-

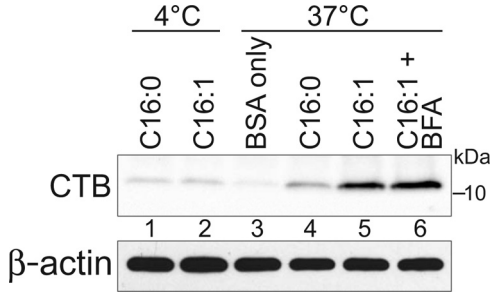

FIGURE 3. **Biochemical quantitation of C16:0/C16:1-GM1 transcytosis.** Apical surfaces of MDCK monolayers were treated as indicated with C16:0-GM1 or C16:1-GM1 (no Alexa label, described under "Experimental Procedures"). CTB was immunoprecipitated from cell lysates, separated by SDS-PAGE, and immunoblotted using anti-CTB pAb (*top panel*). Pre-IP lysates were immunoblotted for β-actin as cell density control (*bottom panel*). Quantitation of CTB bands showed a 3.7- and 2.8-fold increase in *lane 5* as compared with *lane 4* in two independent experiments. The CTB band in *lane 6* was 38 and 44% greater than *lane 5* in two independent experiments. For these measurements, the relevant 4 °C CTB band (*lanes 1* and *2*) was considered as assay background and subtracted from the CTB bands in *lanes 4–6* prior to comparison.

ized cells because the transcytosed fraction of GM1-CTB complexes never traversed the TGN or ER, and inhibition of the retrograde pathway by treatment of cells with BFA enhanced, rather than diminished, transcytosis. That this sorting pathway emerges from the common endosome would be consistent with the transcytotic pathway taken by FcRn during bidirectional Ig transport (7) and with the observed transport of other synthetic sphingolipids across polarized epithelial cells by transcytosis (15, 16).

Our results have implications for the general principles of lipid sorting in mammalian cells. Although we find that the retrograde and transcytotic pathways for GM1-mediated sorting are distinct, the same short-chain C12:0-GM1 and unsaturated C16:1-GM1 ganglioside species are needed for efficient sorting into both pathways. Similarly, in non-polarized cells, we found recently that sorting from early endosomes into the recycling and retrograde pathways was also more efficient for the short- and unsaturated-chain GM1 sphingolipids (1). The saturated C16:0-GM1 and C18:0-GM1 species, in contrast, were directed preferentially to the late endosomes. The shared dependence on short and unsaturated ceramide domains for lipid sorting out of the common/sorting endosome (and away from the lysosome) suggests a common mechanism.

One way membrane lipids are sorted in mammalian cells is by a molecular process in which individual lipids segregate in membranes of different contours and compositions, as determined by the structure of the lipid (molecular shape) and driven by the minimal free energy of the space it occupies in the membrane bilayer (17). Thus, it is possible that the *cis*-unsaturated and short-acyl chain GM1 species, by virtue of their geometry, sort into retrograde, transcytotic, and recycling pathways because they energetically favor partitioning into the curved membrane contours of the narrow-diameter sorting tubules that emanate from the common endosome and feed these destinations. Such a mechanism would also explain why the long-chain saturated GM1 species that favor partitioning into the flat membrane contours of the maturing endosome are directed to the lysosome in non-polarized cells (1) and why charge differences in sphingolipid head groups have little impact on sorting into the transcytotic pathway in polarized epithelia (18).

Lipids, however, can also sort by a cooperative process involving self-assembly into membrane "nanodomains" (*i.e.* lipid rafts) on the basis of lipid-phase behavior and subsequent interactions with other membrane and membrane-associated proteins (19–21). Consistent with the lipid raft model, we found recently, in non-polarized cells, that retrograde trafficking of C16:1-GM1 to the TGN and ER (but not to the recycling or late endosome) depended on the lipid raft-associated protein flotillin 1 (1, 14). In polarized intestinal T84 cells, however, we find evidence for only a marginal effect of flotillin depletion on retrograde transport from the PM to the ER and no clear evidence for flotillin effecting the sorting of GM1 through the transcytotic pathway. Thus, flotillin 1 may act specifically in sorting GM1 from the common endosome retrograde into the TGN/ER. Our studies, however, do not rule out the possibility that the residual flotillin expression (15%) was sufficient to maintain function in transcytosis or that there are redundant transcytotic pathways. It also remains possible that other proteins may assemble with GM1 to direct transcellular sorting by formation of nanodomains according to the lipid raft hypothesis.

The simplest model emerging from these studies is that lipid shape, typified by the *cis*-unsaturated ceramide species, is a common prerequisite for sorting of GM1 out of the degradative pathway and into the recycling, retrograde, and transcytotic pathways. The geometry of the ceramide domain could drive certain glycosphingolipid species to associate more efficiently with the different membrane tubules and buds that emerge from the common sorting endosome and escape lysosomal transport en route to other intracellular destinations. Presumably, additional mechanisms on the basis of local differences in membrane protein and lipid composition would determine the final destination, but it is possible that lipid sorting into the recycling, retrograde, and transcytotic pathways is stochastic and dependent on transport by narrow, high-curvature membrane buds and tubules emerging from the common endosome. Finally, we note that the ability of certain species of GM1 to cross epithelial barriers by absorptive transcytosis has potential clinical relevance, especially with respect to drug delivery across mucosal surfaces.

Acknowledgments—We thank Marian Neutra for critical reading of the manuscript, the Lencer laboratory for helpful discussions, and Wendy Kam and Meredith O'Hear for help with tissue culture.

REFERENCES

1. Chinnapen, D. J., Hsieh, W. T., te Welscher, Y. M., Saslowsky, D. E., Kaoutzani, L., Brandsma, E., D'Auria, L., Park, H., Wagner, J. S., Drake, K. R., Kang, M., Benjamin, T., Ullman, M. D., Costello, C. E., Kenworthy, A. K., Baumgart, T., Massol, R. H., and Lencer, W. I. (2012) Lipid sorting by ceramide structure from plasma membrane to ER for the cholera toxin receptor ganglioside GM1. *Dev. Cell* **23,** 573–586
2. Jobling, M. G., Yang, Z., Kam, W. R., Lencer, W. I., and Holmes, R. K. (2012) A single native ganglioside GM1-binding site is sufficient for cholera toxin to bind to cells and complete the intoxication pathway. *mBio* **3,** e00401–12
3. Wolf, A. A., Jobling, M. G., Saslowsky, D. E., Kern, E., Drake, K. R., Ken-

worthy, A. K., Holmes, R. K., and Lencer, W. I. (2008) Attenuated endocytosis and toxicity of a mutant cholera toxin with decreased ability to cluster ganglioside GM1 molecules. *Infect. Immun.* **76,** 1476–1484
4. Lencer, W. I., Moe, S., Rufo, P. A., and Madara, J. L. (1995) Transcytosis of cholera toxin subunits across model human intestinal epithelia. *Proc. Natl. Acad. Sci. U.S.A.* **92,** 10094–10098
5. Lencer, W. I., Constable, C., Moe, S., Jobling, M. G., Webb, H. M., Ruston, S., Madara, J. L., Hirst, T. R., and Holmes, R. K. (1995) Targeting of cholera toxin and *E. coli* heat labile toxin in polarized epithelia. Role of C-terminal KDEL. *J. Cell Biol.* **131,** 951–962
6. Dickinson, B., Badizadegan, K., Wu, Z., Ahouse, J. C., Zhu, X., Simister, N. E., Blumberg, R. S., and Lencer, W. I. (1999) Bidirectional FcRn-dependent IgG transport in a polarized human intestinal cell line. *J. Clin. Invest.* **104,** 903–911
7. Tzaban, S., Massol, R. H., Yen, E., Hamman, W., Frank, S. R., Lapierre, L. A., Hansen, S. H., Goldenring, J. R., Blumberg, R. S., and Lencer, W. I. (2009) The recycling and transcytotic pathways for IgG transport by FcRn are distinct and display an inherent polarity. *J. Cell Biol.* **185,** 673–684
8. Odorizzi, G., Pearse, A., Domingo, D., Trowbridge, I. S., and Hopkins, C. R. (1996) Apical and basolateral endosomes of MDCK cells are interconnected and contain a polarized sorting mechanism. *J. Cell Biol.* **135,** 139–152
9. Hoekstra, D., Tyteca, D., and van Ijzendoorn, S. C. (2004) The subapical compartment. A traffic center in membrane polarity development. *J. Cell Sci.* **117,** 2183–2192
10. Dunn, K. W., and Maxfield, F. R. (1992) Delivery of ligands from sorting endosomes to late endosomes occurs by maturation of sorting endosomes. *J. Cell Biol.* **117,** 301–310
11. Raiborg, C., and Stenmark, H. (2009) The ESCRT machinery in endosomal sorting of ubiquitylated membrane proteins. *Nature* **458,** 445–452
12. Fujinaga, Y., Wolf, A. A., Rodighiero, C., Wheeler, H., Tsai, B., Allen, L., Jobling, M. G., Rapoport, T., Holmes, R. K., and Lencer, W. I. (2003) Gangliosides that associate with lipid rafts mediate transport of cholera toxin from the plasma membrane to the ER. *Mol. Biol. Cell* **14,** 4783–4793
13. Saslowsky, D. E., and Lencer, W. I. (2008) Conversion of apical plasma membrane sphingomyelin to ceramide attenuates the intoxication of host cells by cholera toxin. *Cell Microbiol.* **10,** 67–80
14. Saslowsky, D. E., Cho, J. A., Chinnapen, H., Massol, R. H., Chinnapen, D. J., Wagner, J. S., De Luca, H. E., Kam, W., Paw, B. H., and Lencer, W. I. (2010) Intoxication of zebrafish and mammalian cells by cholera toxin depends on the flotillin/reggie proteins but not Derlin-1 or -2. *J. Clin. Invest.* **120,** 4399–4409
15. van Ijzendoorn, S. C., Zegers, M. M., Kok, J. W., and Hoekstra, D. (1997) Segregation of glucosylceramide and sphingomyelin occurs in the apical to basolateral transcytotic route in HepG2 cells. *J. Cell Biol.* **137,** 347–357
16. van Ijzendoorn, S. C., and Hoekstra, D. (1998) (Glyco)sphingolipids are sorted in sub-apical compartments in HepG2 cells. A role for non-Golgi-related intracellular sites in the polarized distribution of (glyco)sphingolipids. *J. Cell Biol.* **142,** 683–696
17. Mukherjee, S., Soe, T. T., and Maxfield, F. R. (1999) Endocytic sorting of lipid analogues differing solely in the chemistry of their hydrophobic tails. *J. Cell Biol.* **144,** 1271–1284
18. van Genderen, I., and van Meer, G. (1995) Differential targeting of glucosylceramide and galactosylceramide analogues after synthesis but not during transcytosis in Madin-Darby canine kidney cells. *J. Cell Biol.* **131,** 645–654
19. Lingwood, D., and Simons, K. (2010) Lipid rafts as a membrane-organizing principle. *Science* **327,** 46–50
20. Römer, W., Pontani, L. L., Sorre, B., Rentero, C., Berland, L., Chambon, V., Lamaze, C., Bassereau, P., Sykes, C., Gaus, K., and Johannes, L. (2010) Actin dynamics drive membrane reorganization and scission in clathrin-independent endocytosis. *Cell* **140,** 540–553
21. Sharma, P., Varma, R., Sarasij, R. C., Ira, Gousset, K., Krishnamoorthy, G., Rao, M., and Mayor, S. (2004) Nanoscale organization of multiple GPI-anchored proteins in living cell membranes. *Cell* **116,** 577–589